

Article

Instabilities of the Vortex Lattice and the Peak Effect in Single Crystal $\text{YBa}_2\text{Cu}_4\text{O}_8$

Mehmet Egilmez ^{1,*}, Isaac Isaac ², Ali S. Alnaser ¹, Zbigniew Bukowski ³, Janusz Karpinski ³, Kim H. Chow ² and Jan Jung ²¹ Department of Physics, American University of Sharjah, P.O. Box 26666 Sharjah, UAE² Department of Physics, University of Alberta, Edmonton, AB T6G 2R3, Canada³ Solid State Physics Laboratory, ETH, CH-8093 Zurich, Switzerland

* Correspondence: megilmez@aus.edu

Received: 18 June 2019; Accepted: 30 July 2019; Published: 2 August 2019



Abstract: We report on the measurements of the remnant magnetization, and hence critical current, in a single crystal of $\text{YBa}_2\text{Cu}_4\text{O}_8$. A peak in the temperature dependence of the critical current is observed when the external magnetic field is tilted away from the a–b planes. The observed behavior is attributed to a thermally activated instability-driven vortex-lattice splitting or vortex chain formation. The nature of the peak and the possibility of a thermally-activated dimensional crossover have been discussed.

Keywords: remnant magnetization; vortex-lattice; peak effect

1. Introduction

The properties of vortex-lattice tilted with respect to the CuO_2 planes (the a–b planes) of a layered superconductor have been the subject of intense experimental and theoretical investigations [1,2]. By considering the layered nature of cuprate superconductors, Tachiki and Takahashi [3] were the first to suggest that the modulation of the order parameter perpendicular to the CuO_2 layers can trap the vortices between the layers. The subsequent theoretical works by Feinberg [4] Blatter et al. [5], Ivlev et al. [6], Koshelev [7,8] and Bulaevskii [9] have pointed out that pinning of vortices between the layers occurs only when the angle θ between the CuO_2 planes and the direction of the external magnetic field \mathbf{H} does not exceed a certain critical angle θ_c . Specifically, at small angles of tilt of \mathbf{H} with respect to the a–b planes, the vortex lines are “locked” along the layers and the z-component of the magnetic field (H_z) along the c-axis is screened. When the component of the internal magnetic field along the c-axis exceeds the critical value $H_{\text{lock-in}}$, the vortex lines are “un-locked” and penetration of H_z occurs through the formation of kinks on the vortex lines. The presence of such intrinsic pinning by the layered structure was confirmed by the measurements of the angular dependence of the resistivity in a magnetic field at a temperature close to T_c in a single crystal of $\text{YBa}_2\text{Cu}_3\text{O}_{7-\delta}$ [10].

Theories of the tilted vortex lattice in anisotropic superconductors [11–13] suggest that for a certain range of tilt angles, straight vortex lines parallel to the applied field \mathbf{H} become unstable, leading to the formation of two different types of interpenetrating vortex lines—one oriented approximately parallel to the c-axis and another approximately parallel to the a–b planes. Neither of these two interpenetrating vortex orientations is parallel to the applied field \mathbf{H} . However, the straight vortex lines are stable when the applied field is oriented parallel to the c-axis or the a–b planes. The effect of temperature on the tilted vortex lattice in a layered superconductor has been explored by Machida and Kaburaki [14]. They studied this problem by performing numerical simulations of time-dependent Ginzburg–Landau equations for the layered superconductor, where the unit cell dimension d along the c-axis is larger than the coherence length ξ_c . Their simulations predict that a lattice of tilted straight-vortex lines is

transformed into two vortex sub-lattices. The vortex-line segments reside between the a–b planes in one sub-lattice, and along the c-axis in the other. On the other hand, layered superconductors have a very wide spectrum vortex phase diagram in tilted magnetic fields. Possible structures include the kinked lattice, tilted vortex chains, crossing lattices composed of Josephson vortices, and pancake vortex stacks [8]. Among many possible arrangements, vortex chain formation has been suggested as the most feasible structure for moderately anisotropic layered structures, as vortex dynamics can be well described with continuous anisotropic theory [15].

Experimental studies of such a temperature-induced instability of the vortex lattice are scarce. In this report, we present the experimental observation of a thermally-activated transformation of the vortex lattice at small tilt angles with respect to the a–b planes in a layered superconductor. This transformation results in a peak in the temperature-dependent remnant magnetization that is proportional to the critical current density. The remnant magnetization, that is, the maximum trapped magnetization at which the sample is fully penetrated by the magnetic flux, allows one to determine the maximum density of vortex lines trapped in a superconductor at different temperatures and magnetic fields.

2. Results and Discussion

The measurements of the magnetization along the b- and c-axes (see Figure 1b) revealed that this sample has a T_c of 79.6 K and its diamagnetic response is temperature-independent at temperatures below 60–70 K. Y124 is a naturally under-doped, stoichiometric, and un-twinned cuprate with an anisotropy parameter $\gamma \approx 13$ –15 [16–19], which is about two times higher than $\gamma \approx 7$ for $\text{YBa}_2\text{Cu}_3\text{O}_{7-\delta}$ and much smaller than $\gamma \approx 50$ –200 for $\text{Bi}_2\text{Sr}_2\text{CaCu}_2\text{O}_x$ (BSCCO). Its structure is composed of stacked CuO_2 plane bi-layers (the crystallographic a–b plane) with the unit cell dimension along the c-axis of around 2.7 nm.

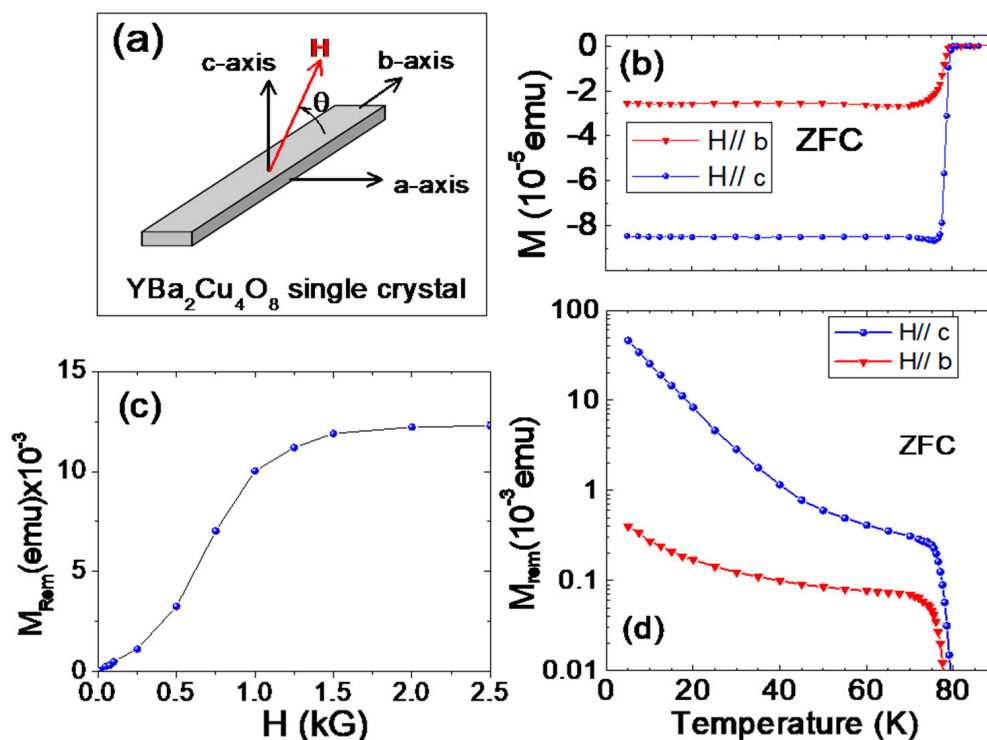


Figure 1. (a) Schematic of the Y124 crystal showing the a–b–c crystallographic axes and the direction of the applied field H; (b) temperature dependence of the zero-field-cooled (ZFC) diamagnetic magnetization of Y124 crystal measured along the c- and b-axes in a field of 2 G; (c) a typical M_{REM} saturation test measurement at 10 K along c-axis; (d) temperature dependence of the ZFC remnant (trapped) magnetization measured along the c- and b-axes.

The measurements of the temperature dependence of the remnant magnetization were done for several different orientations of a magnetic field H : along the b -axis in the a - b planes ($\theta = 0^\circ$); along the c -axis ($\theta = 90^\circ$); and for H tilted towards the c -axis in approximately $2^\circ \mp 0.5^\circ$ increments by the angles θ of 3.5° , 5.5° , and 7.0° with respect to the b -axis. Remnant magnetization can be defined as measured residual magnetization after applied field has been removed. A typical M_{REM} versus applied field dependence is shown in Figure 1c. We have found that an applied field around 2.2 kG is sufficient to saturate M_{REM} at all temperatures and along all crystallographic directions. The temperature dependence of the zero-field-cooled remnant (trapped) magnetization of Y124 for a magnetic field oriented along the b -axis in the a - b plane and along the c -axis are presented in Figure 1d). The high value of the c -axis remnant magnetization results from the strong pinning of vortex lines along the c -axis. For both cases at temperatures below 70 K, the drop of the remnant magnetization (the critical current) with an increasing temperature could be described by the empirical formula $M_{\text{rem}}(T) = ae^{-T/T_0} + b$, where a , b , and T_0 are constants. This empirical relationship is often interpreted as the presence of the pinning centers with small energies [20,21]. An external magnetic field of the order of a few kG was applied to saturate the trapped magnetization along the b - and c -axes at all temperatures (see Figure 1c).

As the angle of the tilt between the b -axis and the applied field H is increased, dramatically different behavior is observed. In particular, there is now an obvious peak in the temperature dependence of the ZFC remnant magnetization (see Figure 2). To our knowledge, this behavior has not been observed before, and is the main result of this paper. The peak's position is the same for 3.5° and 5.5° . Increasing the tilt angle θ from 5.5° to 7.0° causes the onset temperature to decrease and the magnitude of the remnant magnetization to increase. The appearance of the peak in $M_{\text{rem}}(T)$ suggests that the extra vortex-lines are being trapped in the vicinity of the peak's temperature. For 3.5° and 5.5° tilt angles, the magnetization follows the trend of b -axis magnetization below 25 K, while for the 7° tilt angle, the magnetization follows b -axis magnetization at temperatures less than 15 K. We postulate that the formation of the peak at higher temperatures occurs when this vortex lattice becomes unstable and induces formation of additional pinning centers at different angles. These arguments are based on well-established ideas that were developed previously in order to explain the behavior of the tilted vortex lattice in anisotropic superconductors [11–15]. On the other hand, based on Bulaevskii et al. [9], γ for Y124 is too low for a combined lattice scenario [8]. This argument can be supported by the work of Bending and Dodgson, in which the importance of the layered structure in the determination of the vortex matter in reasonably high tilted fields for moderately anisotropic superconductors like Y124 is negligible; hence, vortex chain realization is more likely than a combined lattice formation [15]. For us, however, it is very difficult to interpret our data based on the available theories based on equilibrium vortex dynamics, as our remnant magnetization measurements possibly represents non equilibrium states. The measurements of the remnant magnetization performed for the positive and negative tilt angle θ° with respect to the a - b planes revealed very similar peaks in $M_{\text{rem}}(T)$. We believe, therefore, that the peak originates from vortex-chains trapped by pinning centers most likely along the c -axis (and not by any tilted line defects). The background, on the other hand, could result from the vortex-chains trapped between the a - b planes along the b -axis. We attempted to separate the peaks in $M_{\text{rem}}(T)$ from the background whose temperature dependence has a form similar to that of the remnant magnetization measured along the b -axis, that is, $M_{\text{rem}}(T) = ae^{-T/T_0} + b$. The results are shown in Figure 3.

The fit to these data was carried out by assuming that the peaks are formed by the trapping of vortex segments at a certain angle between the a - b planes and the c -axis. The presence of the peak suggests that the instability could be thermally activated over an effective barrier $E_i - E_v$, where E_i is an intrinsic energy barrier that prevents the formation of the instability and E_v is the energy of a tilted vortex line, which increases with an increasing tilt angle θ [9].

The peak's remnant magnetization $\Delta M_{\text{rem}}(T)$ is proportional to the number of thermally-activated c -axis vortex segments $n(T)$, which increases with temperature according to the following empirical relation:

$$\Delta M_{rem} \propto n(T) = [N(T)]e^{-\frac{(E_i-E_v)}{k_B T}}, \quad (1)$$

where $N(T)$ is the maximum number of the trapped vortex segments, which decreases with temperature. $N(T)$ is proportional to the critical current density in a magnetic field applied at an angle θ with respect to the a–b planes. The temperature dependence of $N(T)$ is assumed to have an exponential form similar to that of the b-axis or c-axis remnant magnetizations, that is,

$$\Delta M_{rem} \propto \left[a e^{-\frac{T}{T_0}} + b \right] e^{-\frac{(E_i-E_v)}{k_B T}}. \quad (2)$$

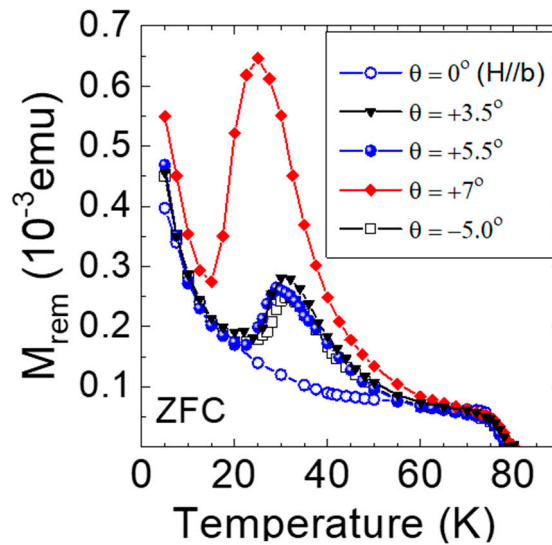


Figure 2. Temperature dependence of the ZFC remnant magnetization measured along the b-axis for $H \parallel b$ and for H tilted towards the c-axis by an angle θ of 3.5°, 5.5°, and 7.0° with respect to the b-axis.

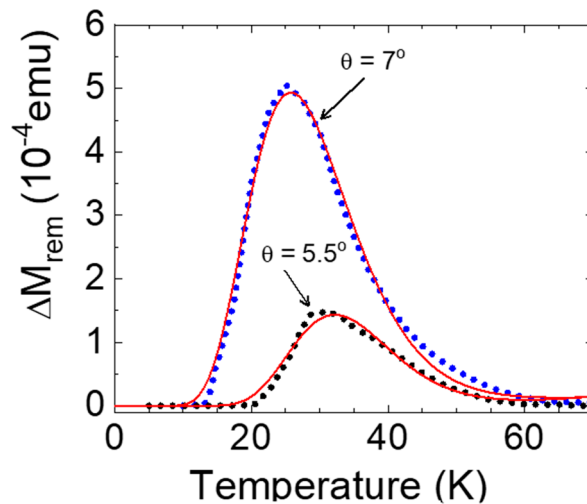


Figure 3. Dotted curves: temperature dependence of the peak’s remnant magnetization obtained by subtracting the background from the remnant magnetization measured for H tilted towards the c-axis by an angle θ of 5.5° and 7.0° with respect to the b-axis (see Figure 2). Solid lines represent the fit to the experimental data using Equation (2).

The fitting of Equation (2) to the experimental data in Figure 3 gives the effective activation energy $\frac{E_{eff}}{k_B} = \frac{(E_i-E_v)}{k_B}$ of 320 ± 10 K for the external fields tilted by the angles 3.5°–5.5° and a smaller one of 150 ± 2 K for fields tilted by 7.0°. E_i could be interpreted as the energy barrier that separates

the free energy minimum of the tilted straight vortex-line lattice from those of the two split vortex sub-lattices or vortex chains. The straight vortex lattice tilted at a certain angle θ appears to be more stable at low temperatures below the peak's maximum. At higher temperatures, however, the two split interpenetrating vortex sub-lattices or vortex chains are more stable, which could be attributed to a loss of the condensation energy between the layers [14] with an increasing temperature. This could cause a shift of the energy minima of the two vortex sub-lattices to below that of the straight vortex-line lattice. On the other hand, when the temperature is fixed, for example, at 20 K (see Figure 4), the straight vortex-line lattice is more stable for tilt angles of 3.5° – 5.5° . Increasing the tilt angle to 7.0° causes an increase of the straight vortex-line energy E_v , and consequently a reduction of the effective energy barrier E_{eff} associated with a shift of the peak to lower temperatures. This could lead to an increase of the energy minimum of the straight vortex-line lattice to above those of the vortex sub-lattices or vortex chains.

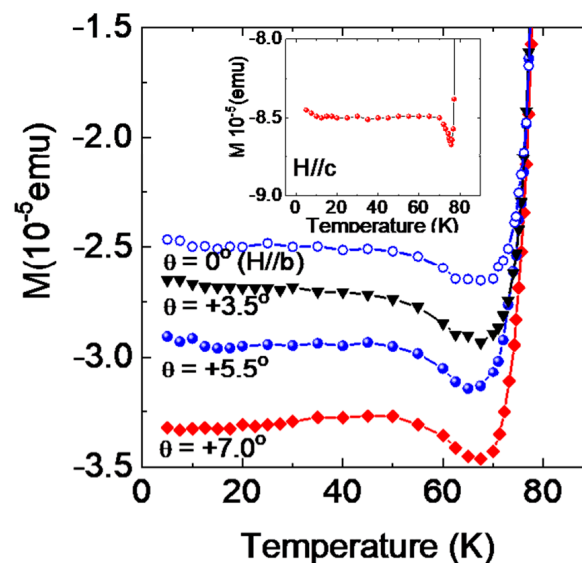


Figure 4. Temperature dependence of the zero-field-cooled (ZFC) diamagnetic magnetization measured in a field of 2 G for \mathbf{H} tilted towards the c -axis by an angle θ of 3.5° , 5.5° , and 7.0° with respect to the b -axis. It shows an enhancement of the magnetization (a “peak effect”) close to T_c . The inset shows the corresponding diamagnetic magnetization measured along the c -axis.

So far, the vortex-tilt induced maxima in the temperature dependence of the remnant magnetization have not been observed in $\text{YBa}_2\text{Cu}_3\text{O}_{7-\delta}$ (Y123) and $\text{Bi}_2\text{Sr}_2\text{CaCu}_2\text{O}_x$ crystals. The anisotropy parameter $\gamma \approx 7$ for Y123 may be too low for the vortex instability to be formed. It is close to the threshold value of the anisotropy parameter necessary to trigger the vortex instability, according to a theory of Sudbo et al. [11]. On the other hand, very high γ for BSCCO crystals could make the vortex lattice splitting energetically favorable at all temperatures. It would be, however, worthwhile to perform new measurements of the temperature dependence of the remnant magnetization for magnetic fields applied at small angles to the a – b planes in these systems as well as in the iron-arsenide based layered superconductors [22].

We would like to note here that there is no direct relationship between the observed tilted vortex-line instability and the anomalous maximum in the temperature dependence of the critical current (known as a “peak effect”), which occurs in the vicinity of the superconductor-to-normal-metal transition in type-II superconductors, such as NbSe_2 and $\text{YBa}_2\text{Cu}_3\text{O}_{7-\delta}$ [23,24]. It is believed that the “peak effect” is the result of a strong vortex pinning induced by the vortex-lattice softening prior to the vortex-lattice melting close to T_c . An increase of the vortex pinning at the “peak” causes a more efficient shielding of the penetrating field by a superconducting sample, which results in the rise of the diamagnetic magnetization. This type of a critical current anomaly is also present in our $\text{YBa}_2\text{Cu}_4\text{O}_8$

crystal (see Figure 4). However, in contrast to the peak caused by the tilted vortex-line instability, the “peak effect” is nearly independent of the magnetic field tilt angle. Another known type of “peak effect” in type-II superconductors is the so-called fishtail effect or second peak in the magnetization. In a typical type-II superconductor, vortex lines penetrating from the surface into the bulk of the material may be trapped at pinning centers, leading to a spatially-inhomogeneous vortex distribution and hence a net magnetization. An increase in the external magnetic field will cause squeezing of the vortex lines; hence, interaction between the vortex lines increases. At large enough fields, such a strong interaction will counteract the pinning forces and results in a decrease in magnetization of the specimen. However, in certain superconductors such as YBCO (Y123) [25], BISCCO [26], iron based superconductors [27], and NbSe₂ [28], the additional increase in the external magnetic field will lead to an increase in the magnetization of the specimen. This behavior is known as a second peak in magnetization or the fish tail effect. The origin of the fish tail effect in type-II superconductors is still under debate. A wide spectrum of vortex dynamical mechanisms including crossover from elastic to plastic (E–P) vortex creep, vortex order–disorder phase transition, vortex lattice structural phase transition (VL), surface barrier, vortex clustering, and so on, were suggested to explain the fish tail effect [29–34]. On the basis of several previous works, we can conclude that the vortex dynamics of Y124 are complex, especially in the 30–60 K range [31,32,35–37]. The shape of the second peak in the magnetization is not typical compared with the ones observed in Y123 (see Figure 5). In this temperature range, the peaks are very asymmetric and the field sweep direction is important. Relevant to our observations, Zech et al. studied the relaxation behavior of the remnant magnetization of the Y124 as a function of orientation angle between the c-axis and ab-plane [35]. This study revealed a prominent 2D to 3D dimensional crossover in the range of 30–60 K [35]. In the low temperature range ($T < 40$ K), remnant magnetization relaxes towards the c-axis direction, irrespective of the rotation angle though a thermally activated process. However, at temperatures higher than 40 K, the system behaves like a 3D anisotropic superconductor and remnant magnetization rotates towards a-b plane. It is noteworthy to mention that the observed peaks in the remnant magnetization of our specimen appear within the temperature range of 30–60 K. Hence, thermally-activated dimensional cross over may play a role in the observed behavior.

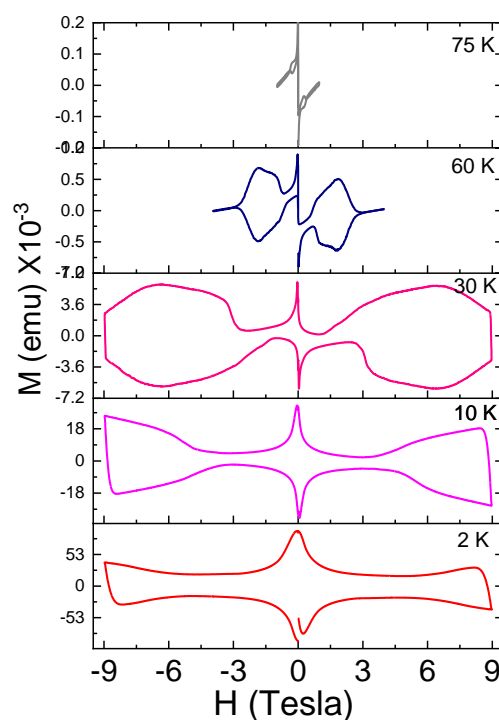


Figure 5. Magnetic field dependence of the magnetization measured along the c-axis at different temperatures.

3. Materials and Methods

The experiments were performed on a crystallographically well-oriented bar-shaped single-crystal of $\text{YBa}_2\text{Cu}_4\text{O}_8$ (Y124). The standard measurements of the temperature dependence of the diamagnetic and the remnant magnetizations were performed with a SQUID magnetometer (Quantum Design) and a vibrating sample magnetometer (VSM). The magnetization was measured in the direction of the applied field. The Y124 single crystal was grown by the high-pressure flux method [15]. A bar-shaped sample with dimensions along the a–b–c axes of approximately $0.5 \times 1.6 \times 0.1 \text{ mm}^3$ (see Figure 1a) was chosen for these studies.

4. Conclusions

In summary, we investigated the peak in the temperature dependence of the remnant magnetization of the Y124 crystal subjected to a magnetic field tilted towards the c-axis at small angles relative to the b-axis (the a–b planes). The peak is absent when the field is oriented along the c- or b-axes. The peak was attributed to the thermally activated vortex-lattice instability that produces vortex segments aligned along the c-axis. In anisotropic superconductors such as the material under study, the relaxation process at arbitrary angles of the external magnetic field (not parallel to the crystallographic axes) is complex because of the temperature-dependent coupling strength between neighboring layers, and hence is difficult to model. We believe that our findings may stimulate the development of theories to explain the effect of temperature on the vortex-matter in tilted magnetic fields.

Author Contributions: Conceptualization, I.I.; Formal analysis, M.E.; Funding acquisition, M.E.; Investigation, Z.B. and K.H.C.; Methodology, Z.B. and J.K.; Project administration, M.E.; Resources, A.S.A., K.H.C. and J.J.; Writing—original draft, M.E. and J.J.; Writing—review & editing, M.E., A.S.A., K.H.C. and J.J.

Funding: M.E. and A.S.A. acknowledge funding from Faculty Research Grant from American University of Sharjah. Grant numbers: FRG17-R-11 & EFRG18-MSE-CAS-68. K.H.C. and J.J. acknowledges support from NSERC.

Conflicts of Interest: The authors declare no conflict of interest.

References

1. Glatz, A.; Vlasko-Vlasov, V.K.; Kwok, W.K.; Crabtree, G.W. Vortex cutting in superconductors. *Phys. Rev. B* **2016**, *94*, 064505. [[CrossRef](#)]
2. Toft-Petersen, R.; Abrahamsen, A.B.; Balog, S.; Porcar, L.; Laver, M. Decomposing the Bragg glass and the peak effect in a Type-II superconductor. *Nat. Commun.* **2018**, *9*, 901. [[CrossRef](#)] [[PubMed](#)]
3. Tachiki, M.; Takahashi, S. Strong vortex pinning intrinsic in high-Tc oxide superconductors. *Solid State Commun.* **1989**, *70*, 291. [[CrossRef](#)]
4. Feinberg, D.; Villard, C. Intrinsic pinning and lock-in transition of flux lines in layered type-II superconductors. *Phys. Rev. Lett.* **1990**, *65*, 919. [[CrossRef](#)] [[PubMed](#)]
5. Blatter, G.; Rhyner, J.; Vinokur, V.M. Vortex pinning by twin boundaries in copper oxide superconductors. *Phys. Rev. B* **1991**, *43*, 7826. [[CrossRef](#)]
6. Ivlev, B.I.; Ovchinnikov, Y.N.; Pokrovsky, V.L. The kinked vortices in layered superconductors in the presence of a tilted magnetic field. *Mod. Phys. Lett. B* **1991**, *5*, 73. [[CrossRef](#)]
7. Koshelev, A.E. Kink walls and critical behavior of magnetization near the lock-in transition in layered superconductors. *Phys. Rev. B* **1993**, *48*, 1180. [[CrossRef](#)]
8. Koshelev, A.E. Vortex-chain phases in layered superconductors. *Phys. Rev. B* **2005**, *71*, 174507. [[CrossRef](#)]
9. Bulaevskii, N.L.; Ledvij, M.; Kogan, V.G. Vortices in layered superconductors with Josephson coupling. *Phys. Rev. B* **1992**, *46*, 366. [[CrossRef](#)]
10. Kwok, W.K.; Welp, U.; Vinokur, V.M.; Fleshler, S.; Downey, J.; Crabtree, G.W. Direct observation of intrinsic pinning by layered structure in single-crystal $\text{YBa}_2\text{Cu}_3\text{O}_{7-\delta}$. *Phys. Rev. Lett.* **1991**, *67*, 390. [[CrossRef](#)]
11. Sudbo, A.; Brandt, E.H.; Huse, D.A. Multiple coexisting orientations of flux lines in superconductors with uniaxial anisotropy. *Phys. Rev. Lett.* **1993**, *71*, 1451. [[CrossRef](#)] [[PubMed](#)]
12. Sardella, E.; Moore, M.A. Tilt-wave instability of the flux-line lattice in anisotropic superconductors. *Phys. Rev. B* **1993**, *48*, 9664. [[CrossRef](#)] [[PubMed](#)]

13. Thompson, A.M.; Moore, M.A. Instabilities in the flux-line lattice of anisotropic superconductors. *Phys. Rev. B* **1997**, *55*, 3856. [[CrossRef](#)]
14. Machida, M.; Kaburaki, H. Structure of flux lines in three-dimensional layered type-II superconductor: Numerical experiments. *Phys. Rev. Lett.* **1995**, *74*, 1434. [[CrossRef](#)] [[PubMed](#)]
15. Bending, S.J.; Dodgson, M.W. Vortex chains in anisotropic superconductors. *J. Phys. Condens. Matter* **2005**, *17*, 955R. [[CrossRef](#)]
16. Karpinski, J.; Kaldis, E.; Jilek, E.; Rusiecki, S.; Bucher, B. Bulk synthesis of the 81-K superconductor $\text{YBa}_2\text{Cu}_4\text{O}_8$ at high oxygen pressure. *Nature* **1988**, *336*, 660. [[CrossRef](#)]
17. Qiu, X.G.; Moshchalkov, V.V.; Bruynseraede, Y.; Karpinski, J. Vortex lattice melting into a disentangled liquid followed by the 3D-2D decoupling transition in $\text{YBa}_2\text{Cu}_4\text{O}_8$ single crystals. *Phys. Rev. B* **1998**, *58*, 8826. [[CrossRef](#)]
18. Iwasawa, H.; Dudin, P.; Inui, K.; Masui, T.; Kim, T.K.; Cacho, C.; Hoesch, M. Buried double CuO chains in $\text{YBa}_2\text{Cu}_4\text{O}_8$ uncovered by nano-ARPES. *Phys. Rev. B* **2019**, *99*, 140510. [[CrossRef](#)]
19. Hussey, N.E.; Takagi, H.; Mori, N.; Takeshita, N.; Iye, Y.; Adachi, S.; Tanabe, K. Vortex Lattice Melting in $\text{YBa}_2\text{Cu}_4\text{O}_8$ with $\text{H}\parallel\text{ab}$. *J. Supercond.* **1999**, *12*, 583. [[CrossRef](#)]
20. Kuznetsov, A.V.; Sannikov, I.I.; Ivanov, A.A.; Menushenkov, A.P. Temperature dependence of the critical current of $\text{YBa}_2\text{Cu}_3\text{O}_{7-\delta}$ films. *JETP Lett.* **2017**, *106*, 324. [[CrossRef](#)]
21. Lairson, B.M.; Sun, J.Z.; Bravman, J.C.; Geballe, T.H. Reduction of the magnetization decay rate in high- T_c superconductors. *Phys. Rev. B* **1990**, *42*, 1008. [[CrossRef](#)] [[PubMed](#)]
22. Kamihara, Y.; Watanabe, T.; Hirano, M.; Hosono, H.J. Iron-Based Layered Superconductor $\text{La}[\text{O}_{1-x}\text{F}_x]\text{FeAs}$ ($x = 0.05\text{--}0.12$) with $T_c = 26$ K. *Am. Chem. Soc.* **2008**, *130*, 3296. [[CrossRef](#)] [[PubMed](#)]
23. Mohan, S.; Sinha, J.; Banerjee, S.S.; Myasoedov, Y. Instabilities in the Vortex Matter and the Peak Effect Phenomenon. *Phys. Rev. Lett.* **2007**, *98*, 027003. [[CrossRef](#)] [[PubMed](#)]
24. Kwok, W.K.; Fendrich, J.A.; van der Beek, C.J.; Crabtree, G.W. Peak Effect as a Precursor to Vortex Lattice Melting in Single Crystal $\text{YBa}_2\text{Cu}_3\text{O}_{7-\delta}$. *Phys. Rev. Lett.* **1994**, *73*, 2614. [[CrossRef](#)] [[PubMed](#)]
25. Kupfer, H.; Wolf, T.; Lessing, C.; Zhukov, A.A.; Lancon, X.L.; Meier-Hirmer, R.; Schauer, W.; Wuhl, H. Peak effect and its evolution from oxygen deficiency in $\text{YBa}_2\text{Cu}_3\text{O}_{7-\delta}$ single crystals. *Phys. Rev. B* **1998**, *58*, 2886. [[CrossRef](#)]
26. Gozzelino, L.; Botta, D.; Chiodoni, A.; Gerbaldo, R.; Ghigo, G.; Laviano, F.; Mezzetti, E. Magneto-optical analysis of second-peak effect in BSCCO single crystals. *Europhys. Lett.* **2002**, *60*, 910. [[CrossRef](#)]
27. Terashima, T.; Kikugawa, N.; Kiswandhi, A.; Choi, Eu.; Kihou, K.; Ishida, S.; Lee, Ch.; Iyo, A.; Eisaki, H.; Uji, S. Anomalous peak effect in iron-based superconductors $\text{Ba}_{1-x}\text{K}_x\text{Fe}_2\text{As}_2$ ($x \approx 0.69$ and 0.76) for magnetic-field directions close to the ab plane and its possible relation to the spin paramagnetic effect. *Phys. Rev. B* **2019**, *99*, 094508. [[CrossRef](#)]
28. Kokubo, N.; Kadowaki, K.; Takita, K. Peak Effect and Dynamic Melting of Vortex Matter in NbSe_2 . *Phys. Rev. Lett.* **2005**, *95*, 177005. [[CrossRef](#)]
29. Abulafia, Y.; Shaulov, A.; Wolfus, Y.; Prozorov, R.; Burlachkov, L.; Yeshurun, Y.; Majer, D.; Zeldov, E.; Wühl, H.; Geshkenbein, V.B. Plastic Vortex Creep in $\text{YBa}_2\text{Cu}_3\text{O}_{7-x}$ Crystals. *Phys. Rev. Lett.* **1996**, *77*, 1596. [[CrossRef](#)]
30. Nishizaki, T.; Naito, T.; Kobayashi, N. Anomalous magnetization and field-driven disordering transition of a vortex lattice in untwinned $\text{YBa}_2\text{Cu}_3\text{O}_y$. *Phys. Rev. B* **1998**, *58*, 11169. [[CrossRef](#)]
31. Rosenstein, B.; Shapiro, B.Y.; Shapiro, I.; Bruckental, Y.; Shaulov, A.; Yeshurun, Y. Peak effect and square-to-rhombic vortex lattice transition in $\text{La}_{2-x}\text{Sr}_x\text{CuO}_4$. *Phys. Rev. B* **2005**, *72*, 144512. [[CrossRef](#)]
32. Kopylov, V.N.; Koshelev, A.E.; Schegolev, F.; Togonidze, T.G. The role of surface effects in magnetization of high- T_c superconductors. *Phys. C* **1990**, *170*, 291. [[CrossRef](#)]
33. Zhou, W.; Xing, X.; Wu, W.; Zhao, H.; Shi, Z. Second magnetization peak effect, vortex dynamics, and flux pinning in 112-type superconductor $\text{Ca}_{0.8}\text{La}_{0.2}\text{Fe}_{1-x}\text{Co}_x\text{As}_2$. *Sci. Rep.* **2016**, *6*, 22278. [[CrossRef](#)]
34. Jackson, D.K.; Nicodemi, M.; Perkins, G.K.; Lindop, N.A.; Jensen, H.J. Vortex clustering: The origin of the second peak in the magnetisation loops of type-two superconductors. *Europhys. Lett.* **2000**, *52*, 210. [[CrossRef](#)]
35. Zech, D.; Keller, H.; Warden, M.; Simmler, H.; Stäuble-Pümpin, B.; Zimmermann, P.; Kaldis, E.; Karpinski, J. Angle-dependent magnetic-relaxation studies in single-crystal $\text{YBa}_2\text{Cu}_4\text{O}_8$. *Phys. Rev. B* **1993**, *48*, 6533. [[CrossRef](#)]
36. Katayama, K.; Yoshida, Y.; Kawamata, S.; Ishida, T.; Shibata, K.; Sasaki, T.; Kobayashi, N.; Adachi, S.; Tajima, S. Peak effect and vortex phase diagram of $\text{YBa}_2\text{Cu}_4\text{O}_8$. *Phys. C* **2003**, *392*, 382. [[CrossRef](#)]

37. Harrison, N.; Vanacken, J.; Lagutin, A.S.; Hrlach, F. Observation of the peak effect at high fields in single crystalline $\text{YBa}_2\text{Cu}_4\text{O}_8$. *Phys. B* **1995**, *211*, 251. [[CrossRef](#)]



© 2019 by the authors. Licensee MDPI, Basel, Switzerland. This article is an open access article distributed under the terms and conditions of the Creative Commons Attribution (CC BY) license (<http://creativecommons.org/licenses/by/4.0/>).